European Journal of Radiology Open 3 (2016) 138–144

Contents lists available at ScienceDirect

European Journal of Radiology Open

journal homepage: www.elsevier.com/locate/ejro

Diffusion-weighted MR imaging of non-complicated hepatic cysts: Value of 3T computed diffusion-weighted imaging

Yuko Nakamura[a,*], Toru Higaki[a], Yuji Akiyama[b], Wataru Fukumoto[a], Kenji Kajiwara[a], Yoko Kaichi[a], Yukiko Honda[a], Daisuke Komoto[a,1], Fuminari Tatsugami[a], Makoto Iida[a], Toshifumi Ohmoto[c], Shuji Date[a,2], Kazuo Awai[a]

[a] Diagnostic Radiology, Hiroshima University, Hiroshima, Japan
[b] Department of Radiology, Hiroshima University Hospital, Hiroshima, Japan
[c] Radiology, Kure City Medical Association Hospital, Kure, Japan

ARTICLE INFO

Article history:
Received 27 June 2016
Received in revised form 30 June 2016
Accepted 2 July 2016
Available online 18 July 2016

Keywords:
Diffusion-weighted imaging
Field strength
Computed diffusion-weighted imaging
Non-complicated hepatic cysts
T2 shine-through effect

ABSTRACT

Purpose: To investigate the utility of computed 3T diffusion-weighted imaging (c-DWI) for the diagnosis of non-complicated hepatic cysts with a focus on the T2 shine-through effect.
Materials and methods: In 50 patients with non-complicated hepatic cysts we acquired one set of DWIs (b-value 0 and 1000 s/mm^2) at 1.5T, and two sets at 3T (b-value 0 and 1000 s/mm^2, TE 70 ms; b-value 0 and 600 s/mm^2, TE 60 ms). We defined the original DWIs acquired with b = 1000 s/mm^2 at 1.5T and 3T as "o-1.5T-1000" and "o-3T-1000". c-DWIs were calculated with 3T DWI at b-values of 0 and 600 s/mm^2. c-DWI with b = 1000 and 1500 s/mm^2 were defined as "c-1000" and "c-1500". Radiologists evaluated the signal intensity (SI) of the cysts using a 3-point score where 1 = not visible, 2 = discernible, and 3 = clearly visible. They calculated the contrast ratio (CR) between the cysts and the surrounding liver parenchyma on each DWIs and recorded the apparent diffusion coefficient (ADC) with a b-value = 0 and 1000 s/mm^2 on 1.5T- and 3T DWIs.
Results: Compared with o-1.5T-1000 DWI, the visual scores of all but the c-1500 DWIs were higher ($p = 0.07$ for c-1500- and $p < 0.01$ for the other DWIs). The CR at b = 1000 s/mm^2 was higher on o-3T-1000- than on o-1.5T-1000- ($p < 0.01$) but not higher than on c-1500 DWIs ($p = 0.96$). The CR at b = 0 s/mm^2 on 3T images with TE 70 ms was higher than on 1.5T images ($p < 0.01$). The ADC value was higher for 3T- than 1.5T images ($p < 0.01$).
Conclusions: Non-complicated hepatic cysts showed higher SI on o-3T-1000- than o-1.5T-1000 DWIs due to the T2-shine through effect. This high SI was suppressed on c-1500 DWIs.

Abbreviations: DWI, diffusion-weighted imaging; MRI, magnetic resonance imaging; SI, signal intensity; HCC, hepatocellular carcinoma; SNR, signal-to-noise ratio; c-DWI, computed diffusion-weighted imaging; T1-WI, T1-weighted MRI; T2-WI, T2-weighted MRI; ADC, apparent diffusion coefficient; CR, contrast ratio.

* Corresponding author at: Diagnostic Radiology, Hiroshim University, 1-2-3 Kasumi, Minami-ku, Hiroshima, Japan.
E-mail addresses: yukon@hiroshima-u.ac.jp (Y. Nakamura), higaki@hiroshima-u.ac.jp (T. Higaki), uakiyama@hiroshima-u.ac.jp (Y. Akiyama), wfukumoto@hiroshima-u.ac.jp (W. Fukumoto), kenkaji@hiroshima-u.ac.jp (K. Kajiwara), kaichi@hiroshima-u.ac.jp (Y. Kaichi), honday@hiroshima-u.ac.jp (Y. Honda), komoto@hiroshima-u.ac.jp (D. Komoto), fuminari@hiroshima-u.ac.jp (F. Tatsugami), edamako@hiroshima-u.ac.jp (M. Iida), oomoto_toshi@kure.hiroshima.med.or.jp (T. Ohmoto), shdate@hiroshima-u.ac.jp (S. Date), awai@hiroshima-u.ac.jp (K. Awai).
[1] Radiology, Hiroshima City Asa Citizens Hospital, Hiroshima, Japan.
[2] Radiology, Hiroshima General Hospital of West Japan Railway Company, Hiroshima, Japan.

http://dx.doi.org/10.1016/j.ejro.2016.07.001

1. Introduction

Diffusion-weighted imaging (DWI) is widely used for magnetic resonance imaging (MRI) of the liver. Malignant lesions tend to be more cellular and typically demonstrate impeded diffusion. Consequently, on images obtained with high b-values the residual signal intensity (SI) of malignant lesions is higher than of the background liver parenchyma. Hepatic DWI has been reported to be useful for the differentiation between metastatic and benign solid hepatic lesions and for estimating the malignancy grade of hepatocellular carcinoma (HCC) [1–4]. While simple, non-complicated hepatic cysts usually show a low to isointense signal on high b-value DWI performed on 1.5T MR scanners [5,6], when 3T scanners are used their SI may be high, rendering the diagnosis of hepatic lesions difficult. The SI difference on images acquired at different magnetic field strengths may be attributable to the contribution of T2 hyperintensity to the overall SI on DWI scans. This phenomenon, known as the T2 shine-through effect [7], is effectively controlled on higher b-value images or images acquired with a shorter TE [8,9]. However, DWI performed with high b-values results in an inherently low signal-to-noise ratio (SNR) and is prone to severe distortions of the eddy current by the large diffusion-sensitizing gradients used. It is also difficult to shorten the TE for high b-value images. The image quality of abdominal DWI scans was worse at 3T than 1.5T [10] and the acquisition of diagnostic scans at abdominal 3T DWI with a shorter TE or higher b-value remains difficult.

Computed DWI (c-DWI) is a mathematical computation technique that evaluates DWIs acquired with any b-value. It uses at least two DWI scans obtained with different b-values [11]. By c-DWI higher DWI can be simulated from lower b-value images with a shorter TE without image quality degradation because c-DWI can suppress the background noise while maintaining the original lesion signal [11]. Its utility for the detection of prostate cancer has been reported [12,13]. Thus, c-DWI may help to suppress the T2 shine-through effect on 3T images of non-complicated hepatic cysts if higher b-value images can be simulated from lower b-value images with shorter TE.

The purpose of this study was to clarify the SI difference of DWIs of non-complicated hepatic cysts performed with different magnetic field strengths and to investigate the utility of c-DWI for the diagnosis of non-complicated hepatic cysts scanned at 3T with a focus on the T2 shine-through effect.

2. Materials and methods

This retrospective study was approved by our institutional review board; prior informed patient consent was waived because this study was retrospective observation study. Patient records and information were anonymized and de-identified prior to analyses.

2.1. Study population

All patients underwent 3T MRI studies between January 2013 and March 2015.

Our inclusion criteria were the availability of hepatic MRI scans acquired at both 1.5T and 3T and an imaging diagnosis of non-complicated, non-infectious hepatic cysts larger than 10 mm in diameter. The mean interval between the acquisition of 1.5T and 3T MRI scans was 23.1 months (range 9–68 months). We only evaluated non-complicated hepatic cysts larger than 10 mm in diameter to avoid the partial volume effect because the section thickness and gap of our 1.5T DWI protocol were 8 mm and 2 mm, respectively (see 2.3 Imaging techniques). Of our 50 patients 35 were male and 15 were female; their age ranged from 48 to 89 years (mean 69.9 years). They underwent hepatic MRI studies to screen for HCC due to chronic hepatitis (n = 13), at follow-up after HCC treatment (n = 29), and at follow-up for focal hepatic lesions such as early HCC (n = 8).

2.2. Reference standards

It is difficult to establish histopathologic findings as the reference standard for non-complicated hepatic cysts because they are benign. Therefore, our diagnosis of uncomplicated non-infectious hepatic cysts was based on imaging studies. An uncomplicated non-infectious hepatic cyst was diagnosed if all of the following criteria were met: (a) a homogenous hypo-attenuated lesion on unenhanced CT scans, (b) with no enhancement of the cyst wall and the cystic content on enhanced CT scans, (c) homogenous very low SI on T1-weighted MRI (T1-WI), (d) homogenous very high SI on T2-weighted MRI (T2-WI) [14,15], (e) the absence of enhancement of the cyst wall or cystic content on dynamic gadoxetate disodium (EOB-Primovist, Bayer Yakuhin Ltd., Osaka, Japan)-enhanced MRI scans including the hepatobiliary phase, and (f) the lesion remained unchanged for more than 6 months to avoid the inclusion of patients with infectious or malignant hepatic cystic lesions [16,17].

2.3. Imaging techniques

2.3.1. MRI

We used a 1.5T scanner and an 8-channel body phased array coil (Signa EXCITE HD, GE Healthcare, Milwaukee, WI, USA) and a 3T scanner and an 8-channel body coil plus a 4-channel flex coil (Vantage Titan 3T, Toshiba Medical Systems, Ohtawara, Japan). We acquired one set of 1.5T DWIs (b-value 0 and 1000 s/mm^2) and two sets of 3T DWIs (b-value 0 and 1000 s/mm^2, TE 70 ms; b-value 0 and 600 s/mm^2, TE 60 ms). For 3T scanning we selected a b-value of 1000 s/mm^2, the same b-value applied for 1.5T scans, and 600 s/mm^2 as the highest b-value with TE 60 ms on our scanner. For the creation of c-DWIs we used DWIs acquired with a b-value of 0 and 600 s/mm^2 at 3T.

The scanning parameters for 1.5T imaging were TR/TE 6000 ms/74 ms, echo train length 192, slice thickness 8 mm, gaps 2 mm, matrix size 128 × 192, parallel imaging factor 2, receiver bandwidth 1953.12 Hz per pixel, number of excitations 6, b-value 0 and 1000 s/mm^2. For 3T scanning they were TR/TE 6666 ms/70 ms, echo train length 48, slice thickness and gap 8/2 mm, matrix size 128 × 192, parallel imaging factor 3, receiver bandwidth 1953 Hz per pixel, number of excitations 3, b-value 0 and 1000 s/mm^2, and TR/TE 6666 ms/60 ms, echo train length 48, slice thickness and gap 8/2 mm, matrix size 128 × 192, parallel imaging factor 3, receiver bandwidth 1953 Hz per pixel, number of excitations 3, b-value 0 and 600 s/mm^2.

T1- and T2-weighted- and dynamic MRI scans using gadoxetate disodium were evaluated only to confirm that the hepatic lesions fulfilled the criteria of uncomplicated non-infectious hepatic cysts (see 2.2. Reference standards).

2.3.2. c-DWI

For c-DWI processing we used only 3T images with a b-value of 0 and 600 s/mm^2 and TE 60 ms. All c-DWI were generated using a software program (computed DWI; Toshiba Medical Systems, Ohtawara, Japan) [11,12]. Briefly, first the apparent diffusion coefficient (ADC) was calculated with $ADC = \text{in}[-S_{600}/S_0]/(b_{600} - b_0)$, using two measured DWI signals; S_{600} is the SI at a b-value of 600 s/mm^2 and S_0 is the b-value of 0 s/mm^2, based on a mono-exponential model. ADC maps were constructed using this equation and a voxel-wise calculation. Then the c-DWI signal at $b = b_c$ was obtained with the equation $S_c = S_0 \times \exp[-(b_c - b_0)ADC]$ (Fig. 1)

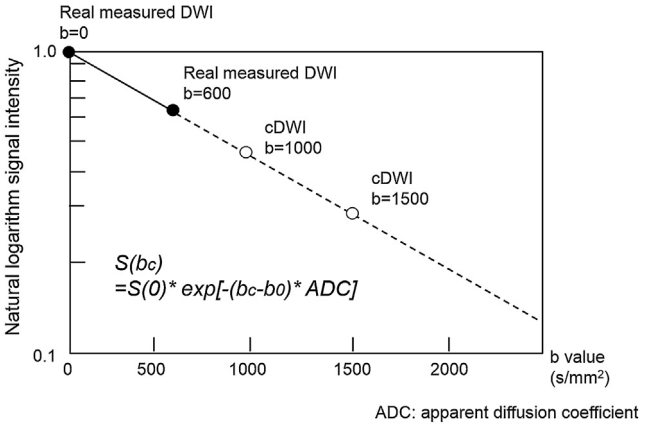

Fig. 1. Schema of the c-DWI procedure.

[11]. c-DWI with b-values of 1000 and 1500 s/mm^2 were generated. The time for generating c-DWI was less than one minute.

2.4. Image analysis

2.4.1. Qualitative analysis

Two board-certified radiologists with 11 and 22 years of experience with abdominal MRI independently evaluated the SI of the hepatic cysts. Disagreements were resolved by consensus. In patients with multiple lesions we evaluated the largest lesion to avoid statistical clustering effects [18]. We defined the original DWIs acquired with b = 1000 s/mm^2 at 1.5T and 3T as "o-1.5T-1000" and "o-3T-1000", respectively, and the c-DWIs at b = 1000 and b = 1500s/mm ^{2} as "c-1000", and "c-1500", respectively.

The two radiologists visually evaluated the SI of the hepatic cysts on all images using a 3-point score where 1 = not visible, 2 = cyst discernible (high SI compared to the surrounding liver parenchyma), and 3 = cyst clearly visible.

2.4.2. Quantitative analysis

The radiologist with 11 years of experience evaluated the size of the hepatic cyst and the contrast ratio (CR) between the cyst and the surrounding liver parenchyma on each DWI using the equation: CR = SI of the hepatic cyst/SI ofthe surrounding liverparenchyma [6]. The radiologist also calculated the CR between the cyst and the surrounding liver parenchyma on DWIs acquired with b = 0 s/mm^2 at 1.5T, and at 3T with TE 70- and TE 60 ms because we suspected cysts to show high SI on 3T DWI due to the T2 shine-through effect [7]. The ADC values of the hepatic cysts were also calculated with a mono-exponential model using b values of 0 and 1000 s/mm^2 for 1.5T DWI and 3T DWI with TE 70 ms.

2.5. Statistical analysis

We only evaluated hepatic cysts larger than 10 mm in diameter to avoid the partial volume effect. However, partial volume effect cannot be excluded completely especially for the lesion smaller than twice the slice thickness. Thus, we also performed subset analysis based on the size of cyst using 20 mm thresholds.

For qualitative analysis we used the two-sided Wilcoxon signed rank test. For quantitative analysis we recorded the statistical differences in the CR of all DWIs using Dunnett's multiple comparisons. Differences in the CR on b = 0 s/mm^2 DWIs were submitted to the Tukey test. Differences in the ADC of the hepatic cysts were tested with the two-sided paired *t*-test. All statistical analyses were performed using free statistical software (R version 2.15.0).

Differences of $p < 0.05$ and of $p < 0.013$ for multiple comparisons of non-parametric data using the Bonferroni correction were considered significant.

3. Results

The mean diameter of the hepatic cysts was 16.1 mm (range 10–62 mm); 28 were in the right- and 22 were in the left lobe. The visual score for cysts on the different images is shown in Table 1; it was 1.00, 1.64, 1.44, and 1.08, respectively, for o-1.5T-1000-, o-3T-1000-, c-1000-, and c-1500 DWIs. Only the difference between o-1.5T-1000 and c-1500 DWIs was not significant ($p = 0.07$); the difference between o-1.5T-1000- and the other images was significant ($p < 0.01$) (Fig. 2).

The results of our subset quantitative analysis based on the size of cysts are shown in Table 2 and 3. The visual score for cysts smaller than 20 mm on the different images is shown in Table 2; it was 1.00, 1.57, 1.43, and 1.08, respectively, for o-1.5T-1000-, o-3T-1000-, c-1000-, and c-1500 DWIs. Only the difference between o-1.5T-1000 and c-1500 DWIs was not significant ($p = 0.11$); the difference between o-1.5T-1000- and the other images was significant ($p < 0.01$). The visual score for cysts larger than 20 mm on the different images is shown in Table 3; it was 1.00, 1.85, 1.46, and 1.08, respectively, for o-1.5T-1000-, o-3T-1000-, c-1000-, and c-1500 DWIs. The difference between o-1.5T-1000 and c-1500 DWIs was not significant ($p = 0.32$). Visual scores for cysts on c-1000- tended to be higher compared to those on o-1.5T-1000 DWIs, but not significant ($p = 0.04$); the difference between o-1.5T-1000- and o-3T-1000 DWIs was significant ($p < 0.01$).

The mean CR value on o-1.5T-1000-, o-3T-1000-, c-1000-, and c-1500 DWIs was 0.98 ± 0.25, 1.45 ± 1.04, 1.31 ± 0.89, and 0.83 ± 0.96, respectively; it was significantly higher on o-3T-1000- than o-1.5T-1000 DWIs ($p < 0.01$). No significant difference was

Table 1
Visual scores of non-complicated hepatic cysts on o-1.5T-1000-, o-3T-1000-, c-1000-, and c-1500 DWIs.

Visual score	o-1.5T-1000	o-3T-1000	c-1000	c-1500
3	0	4	5	0
2	0	24	12	4
1	50	22	33	46
Mean (SD)	1.00 (0.00)	1.64 (1.63)	1.44 (0.67)	1.08 (0.27)

SD: standard deviation.

Table 2
Visual scores of non-complicated hepatic cysts smaller than 20 mm on o-1.5T-1000-, o-3T-1000-, c-1000-, and c-1500 DWIs.

Visual score	o-1.5T-1000	o-3T-1000	c-1000	c-1500
3	0	2	4	0
2	0	17	8	3
1	37	18	25	34
Mean (SD)	1.00 (0.00)	1.57 (0.60)	1.43 (0.69)	1.08 (0.28)

SD: standard deviation.

Table 3
Visual scores of non-complicated hepatic cysts larger than 20 mm on o-1.5T-1000-, o-3T-1000-, c-1000-, and c-1500 DWIs.

Visual score	o-1.5T-1000	o-3T-1000	c-1000	c-1500
3	0	2	1	0
2	0	17	4	1
1	13	4	8	12
Mean (SD)	1.00 (0.00)	1.85 (0.69)	1.46 (0.66)	1.08 (0.28)

SD: standard deviation.

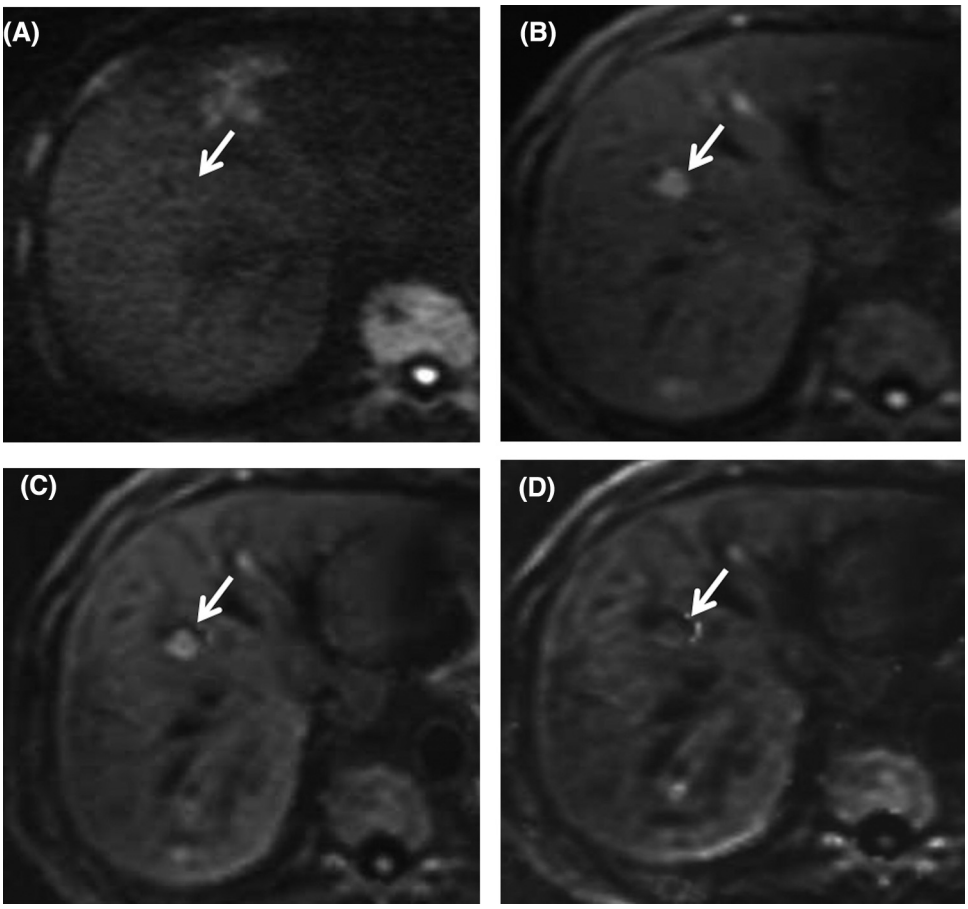

Fig. 2. Hepatic cyst in an 80-year-old man. (A) o-1.5T-1000-, (B) o-3T-1000-, (C) c-1000-, (D) c-1500 DWIs. The cyst (arrow) was isointense on o1.5T-1000-, showed mild high signal intensity on o-3T-1000- and c-1000-, and was isointense on c-1500 DWI.

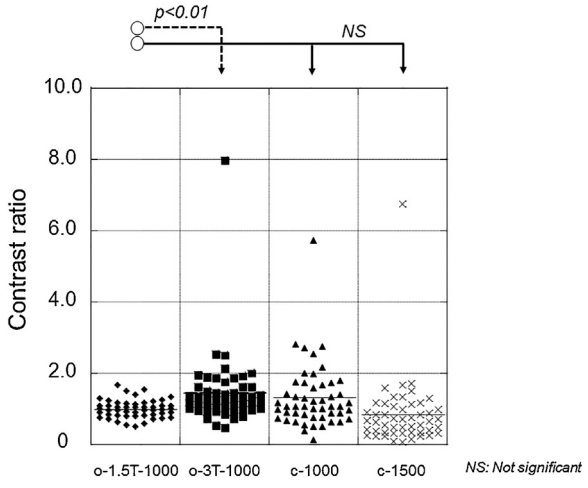

Fig. 3. Contrast ratio (CR) of non-complicated hepatic cysts on o-1.5T-1000-, o-3T-1000-, c-1000-, and c-1500 DWIs. The solid line indicates the mean CR value in each group. The CR was higher on o-3T-1000- than on o-1.5T-1000 DWI ($p < 0.01$). No significant difference was found between o-1.5T-1000- and c-1000 images ($p = 0.07$). There was no significant difference between o-1.5T-1000- and c-1500 DWIs ($p = 0.96$).

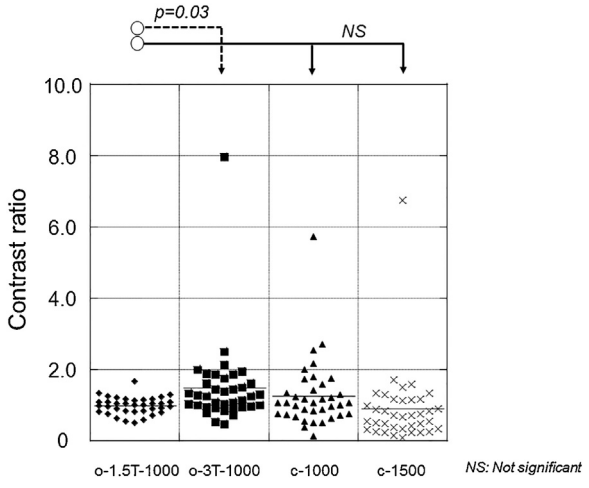

Fig. 4. Contrast ratio (CR) of non-complicated hepatic cysts smaller than 20 mm on o-1.5T-1000-, o-3T-1000-, c-1000-, and c-1500 DWIs. The solid line indicates the mean CR value in each group. The CR was higher on o-3T-1000- than on o-1.5T-1000 DWI ($p = 0.03$). No significant difference was found between o-1.5T-1000- and c-1000 images ($p = 0.22$). The difference between o-1.5T-1000- and c-1500 images was not significant ($p = 0.86$).

found between o-1.5T-1000- and c-1000 images ($p = 0.07$). The difference between o-1.5T-1000- and c-1500 images was not significant ($p = 0.96$) (Fig. 3).

The results of our subset quantitative analysis based on the size of cysts are shown in Figs. 4 and 5. For cysts smaller than 20 mm the mean CR value on o-1.5T-1000-, o-3T-1000-, c-1000-, and c-1500 DWIs was 0.98 ± 0.24, 1.48 ± 1.19, 1.26 ± 0.95, and 0.89 ± 1.09, respectively; it was significantly higher on o-3T-1000- than o-1.5T-1000 DWIs ($p = 0.03$). No significant difference was found between o-1.5T-1000- and c-1000 images ($p = 0.22$). The

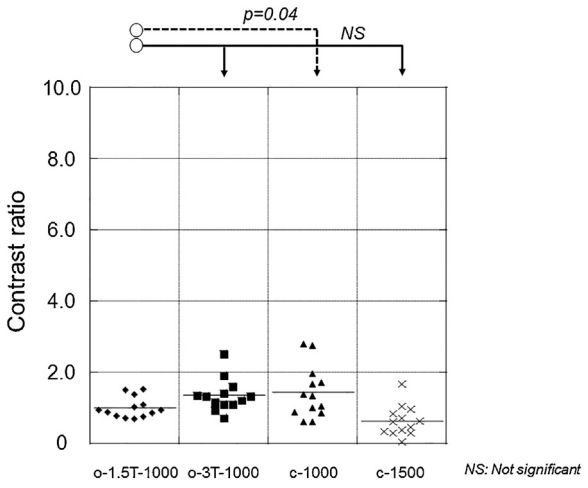

Fig. 5. Contrast ratio (CR) of non-complicated hepatic cysts larger than 20 mm on o-1.5T-1000-, o-3T-1000-, c-1000-, and c-1500 DWIs. The solid line indicates the mean CR value in each group. The CR on o-3T-1000- tended to be higher compared to that on o-1.5T-1000 DWIs, but not significant ($p = 0.08$). The CR was significantly higher on c-1000- than o-1.5T-1000 DWIs ($p = 0.04$). The difference between o-1.5T-1000- and c-1500 images was not significant ($p = 1.00$).

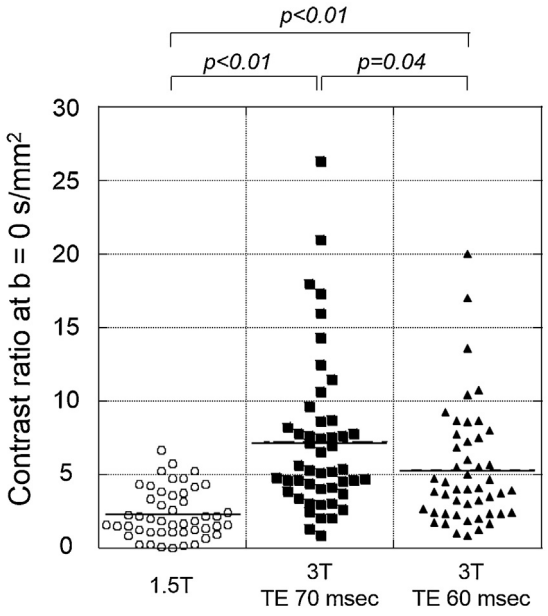

Fig. 6. Contrast ratio of non-complicated hepatic cysts on images obtained with $b = 0\ s/mm^2$ at 1.5T and 3T (TE = 60 and 70 ms). The solid line indicates the mean CR value in each group. The CR was higher on 3T images with TE 70 ms and 60 ms than on 1.5T DWIs ($p < 0.01$) and significantly lower on 3T scans with TE 60 ms than TE 70 ms ($p = 0.04$).

difference between o-1.5T-1000- and c-1500 images was not significant ($p = 0.86$) (Fig. 4). For cysts larger than 20 mm the mean CR value on o-1.5T-1000-, o-3T-1000-, c-1000-, and c-1500 DWIs was 1.01 ± 0.29, 1.37 ± 0.46, 1.44 ± 0.73, and 0.64 ± 0.42, respectively; the CR on o-3T-1000- tended to be higher compared to that on o-1.5T-1000 DWIs, but not significant ($p = 0.08$). The CR was significantly higher on c-1000- than o-1.5T-1000 DWIs ($p = 0.04$). The difference between o-1.5T-1000- and c-1500 images was not significant ($p = 1.00$) (Fig. 5).

The mean CR value of non-complicated hepatic cysts on $b = 0\ s/mm^2$ images acquired at 1.5T and 3T images with TE 60 and 70 ms was 3.41 ± 1.72, 6.39 ± 4.00 and 8.57 ± 5.44, respectively. The CR value at 3T with TE 60 and 70 ms was higher than at 1.5T ($p < 0.01$); at 3T with TE 60 ms it was significantly lower than at 3T with TE 70 ms ($p = 0.04$) (Fig. 6). The ADC value of images acquired at 1.5T and 3T with a b-value of 0 and 1000 s/mm^2 was 2.47 ± 0.52 and $2.76 \pm 0.57 \times 10^{-3}\ mm^2/s$, respectively. It was significantly higher at 3T than at 1.5T ($p < 0.01$).

4. Discussion

We found that the visual score of hepatic cysts was significantly higher on o-3T-1000- than o-1.5T-1000 DWIs regardless of the size of cysts. Quantitative analysis showed that the CR was significantly larger on o-3T-1000- than o-1.5T-1000 DWIs. Based on the results of subset analysis the CR for cysts smaller than 20 mm was also larger on o-3T-1000- than o-1.5T-1000 DWIs with significant difference while the CR for cysts larger than 20 mm o-3T-1000- tended to be higher than that on o-1.5T-1000 DWIs but did not reach significant difference. The CR of cysts at $b = 0\ s/mm^2$ was significantly larger on 3T images with TE 70 ms than on 1.5T images and the ADC values on 3T images acquired at b = 0 and 1000 s/mm^2 were significantly higher than on 1.5T images. Therefore we concluded that the high SI of non-complicated hepatic cysts on 3T DWI is attributable to a larger T2 shine-through effect.

To control the T2 shine-through effect at 3T DWI we created cDWIs using images with a shorter TE (60 ms) and b = 0 and 600 s/mm^2. The visual score assigned to o-1.5-1000- and c-1000 DWIs was different, however, no significant difference was found in their CR although the CR was significantly larger on o-3T-1000- than o-1.5T-1000 DWIs. Based on the results of subset analysis the visual score on c-1000- was higher than that to on o-1.5-1000 DWIs for cysts smaller than 20 mm and also tended to be higher for cysts larger than 20 mm. For the difference in CR between o-1.5-1000- and c-1000 DWIs no significant difference was found for cysts smaller than 20 mm while the CR for cysts larger than 20 mm c-1000- was higher than that on o-1.5T-1000 DWIs with significant difference. The CR on 3T images acquired at $b = 0\ s/mm^2$ was lower at TE 60 ms than TE 70 ms, resulting in a decrease in the T2 shine-through effect. Thus, our findings suggest that the CR on c-1000 DWI may be decreased due to lower T2 shine-through effects, even when the b-value is the same as on o-3T-1000 DWI.

The visual scores assigned to c-1500 and o-1.5T-1000 DWIs were similar regardless of the size of cysts. Quantitative analysis showed that there was no significant difference in the CR on o-1.5T-1000- and c-1500 DWIs. The qualitatively and quantitatively greater SI suppression observed on c-1500 DWIs may be due to their higher b-value than on c-1000 DWIs. At 1.5T, non-complicated simple cysts show a low- to isointense signal on DWI [5,6]. For a correct clinical diagnosis, these cysts should be low- to isointense even on 3T DWI. We suggest that for the evaluation of non-complicated hepatic cysts on 3T scans, c-1500- is more appropriate than o-3T-1000 DWI because, due to control of the T2-shine-through effect, the SI was qualitatively and quantitatively similar on c-1500- and o-1.5T-1000 DWIs.

There are two problems with c-DWI in our study. First we did not to take into account the effect of perfusion-related diffusion; our c-DWI results were based on a mono- rather than a bi-exponential model and the former does not consider the effect of perfusion, indicating that our c-DWI results may have affected not only the true molecular- but also the perfusion-related diffusion [11,12,19,20].

Another problem we encountered with c-DWI was misregistration. Imaging with two or more b-values makes it possible to calculate the ADC of tissues on a voxel-by-voxel basis. However, it is not possible to acquire DWI scans using different b-values for identical slices because the hepatic parenchyma rotates with

respiratory motion [21,22]. Consequently, the ADC at different b-values may not accurately reflect the true value and this may lead to inaccurate c-DWI findings. We are in the process of developing a registration technique to compensate for differences at different b-values.

Our study has some limitations. As our study population was relatively small and the study was retrospective and carried out at a single institution, our findings are preliminary. Second, for the diagnosis of non-complicated hepatic cysts, enhanced CT-, T1-WI-, T2-WI-, and enhanced MRI findings are useful [14,15] although using these imaging techniques, infectious or malignant lesions may show up as cystic lesions [16,17]. On this point, DWI has been reported to be helpful for the diagnosis of infectious or malignant cystic lesions [6,17,23] and DWI studies may be needed for their assessment. Third, ADC maps may be more useful than c-DWI to evaluate the T2 shine-through effect. However, c-DWI allows imaging with higher b-values and can yield more information than simple ADC maps. Moreover, image contrast and thus the lesion conspicuity is markedly lower on ADC maps than on DWIs. Therefore, it may be helpful to add c-DWI to original DWI or ADC maps in the clinical setting. Fourth, voxel-wise c-DWI reported by Gatidis et al. [24] may be a promising approach for the reduction of T2 shine-through effects. However, voxel-wise c-DWI is a complex method that may not find wide application. Fifth, we created c-DWI with only b-values of 1000 and 1500 s/mm^2 although much higher b-values may yield better results. However, higher b-value images result in a poor SNR and more studies are needed to identify the optimal b-value for the diagnosis of non-complicated hepatic cysts on 3T images. Sixth, we used a different TE (60 ms) on 3T DWIs acquired with a b-value 0 and 600 s/mm^2 to reduce the T2 shine-through effect. The relative signal changes in the surrounding liver parenchyma and in the cysts at different TE, b-values, and field strengths are complex and a single relative measurement like the CR may not separate these effects accurately. Moreover, it may be difficult to suppose which, shortening TE or increment of b-value, could control T2-shine through effect effectively. Seventh, we performed DWI scanning after the delivery of gadoxetate disodium and its uptake may affect the SI on DWIs. However, we think that uptake in the liver parenchyma had a negligible effect on the diffusion SI because the values of parameters related to diffusion weighting showed no significant difference before and after gadoxetate disodium administration [25]. Eighth, respiration triggered approach for DWI scanning synchronizes the image acquisition with the patient's breathing cycle and acquires the imaging data during the end expiratory phase to avoid motion artifacts [5]. Indeed, our DWI scanning was performed using this respiration triggered approach. However, technical advances such as navigator based triggering have been recently implemented to improve image quality and to reduce acquisition time [26–28]. Thus, comparison of the image quality of each c-DWI created from DWIs with different respiration triggered approaches might be an interesting next project. Ninth, we only evaluated non-complicated hepatic cysts larger than 10 mm in diameter to avoid the partial volume effect. However, respiratory-triggered DWI has been reported to be helpful to characterize focal liver lesions, even when the diameter of lesions is 10 mm or less [29]. Further investigation may be needed for non-complicated hepatic cysts smaller than 10 mm using the protocol with thinner section thickness and gap. Finally, our c-DWI setting was adapted only for non-complicated hepatic cysts. Other optimal c-DWI settings must be established for the 3T scanning of other hepatic tumors.

In conclusion, our preliminary findings suggest that non-complicated hepatic cysts showed high SI on o-3T-1000 DWI because of the T2 shine-through effect. Such high SI is effectively suppressed on c-1500 DWIs, indicating that c-DWI is useful for control of the T2 shine-through effect.

Conflict of interest

None.

Funding

This research did not receive any specific grant from funding agencies in the public, commercial, or not-for-profit sectors.

Acknowledgement

None.

References

[1] M.L. Testa, R. Chojniak, L.S. Sene, A.S. Damascena, M.D. Guimaraes, J. Szklaruk, et al., Is DWI/ADC a useful tool in the characterization of focal hepatic lesions suspected of malignancy? PLoS One 9 (2014) e101944.
[2] A. Muhi, T. Ichikawa, U. Motosugi, K. Sano, M. Matsuda, T. Kitamura, et al., High-b-value diffusion-weighted MR imaging of hepatocellular lesions: estimation of grade of malignancy of hepatocellular carcinoma, J. Magn. Reson. Imaging 30 (2009) 1005–1011.
[3] T. Parikh, S.J. Drew, V.S. Lee, S. Wong, E.M. Hecht, J.S. Babb, et al., Focal liver lesion detection and characterization with diffusion-weighted MR imaging: comparison with standard breath-hold T2-weighted imaging, Radiology 246 (2008) 812–822.
[4] B. Taouli, D.M. Koh, Diffusion-weighted MR imaging of the liver, Radiology 254 (2010) 47–66.
[5] S. Naganawa, H. Kawai, H. Fukatsu, Y. Sakurai, I. Aoki, S. Miura, et al., Diffusion-weighted imaging of the liver: technical challenges and prospects for the future, Magn. Reson. Med. Sci. 4 (2005) 175–186.
[6] N. Inan, A. Arslan, G. Akansel, Y. Anik, H.T. Sarisoy, E. Ciftci, et al., Diffusion-weighted imaging in the differential diagnosis of simple and hydatid cysts of the liver, AJR Am. J. Roentgenol. 189 (2007) 1031–1036.
[7] J.H. Burdette, A.D. Elster, P.E. Ricci, Acute cerebral infarction: quantification of spin-density and T2 shine-through phenomena on diffusion-weighted MR images, Radiology 212 (1999) 333–339.
[8] S. Feuerlein, S. Pauls, M.S. Juchems, T. Stuber, M.H. Hoffmann, H.J. Brambs, et al., Pitfalls in abdominal diffusion-weighted imaging: how predictive is restricted water diffusion for malignancy, AJR Am. J. Roentgenol. 193 (2009) 1070–1076.
[9] D.M. Koh, D.J. Collins, Diffusion-weighted MRI in the body: applications and challenges in oncology, AJR Am. J. Roentgenol. 188 (2007) 1622–1635.
[10] A.B. Rosenkrantz, M. Oei, J.S. Babb, B.E. Niver, B. Taouli, Diffusion-weighted imaging of the abdomen at 3. 0 Tesla: image quality and apparent diffusion coefficient reproducibility compared with 1. 5 Tesla, J. Magn. Reson. Imaging 33 (2011) 128–135.
[11] M.D. Blackledge, M.O. Leach, D.J. Collins, D.M. Koh, Computed diffusion-weighted MR imaging may improve tumor detection, Radiology 261 (2011) 573–581.
[12] Y. Ueno, S. Takahashi, K. Kitajima, T. Kimura, I. Aoki, F. Kawakami, et al., Computed diffusion-weighted imaging using 3-T magnetic resonance imaging for prostate cancer diagnosis, Eur. Radiol. 23 (2013) 3509–3516.
[13] M.C. Maas, J.J. Futterer, T.W. Scheenen, Quantitative evaluation of computed high B value diffusion-weighted magnetic resonance imaging of the prostate, Invest. Radiol. 48 (2013) 779–786.
[14] K.J. Mortele, P.R. Ros, Cystic focal liver lesions in the adult: differential CT and MR imaging features, Radiographics 21 (2001) 895–910.
[15] D. Mathieu, V. Vilgrain, A.E. Mahfouz, M.C. Anglade, M.P. Vullierme, A. denys benign liver tumors, Magn. Reson. Imaging Clin. N. Am. 5 (1997) 255–288.
[16] A. Bakoyiannis, S. Delis, C. Triantopoulou, C. Dervenis, Rare cystic liver lesions: a diagnostic and managing challenge, World J. Gastroenterol. 19 (2013) 7603–7619.
[17] F. Becce, A. Pomoni, E. Uldry, N. Halkic, P. Yan, R. Meuli, et al., Alveolar echinococcosis of the liver: diffusion-weighted MRI findings and potential role in lesion characterisation, Eur. J. Radiol. 83 (2014) 625–631.
[18] M. Gonen, K.S. Panageas, S.M. Larson, Statistical issues in analysis of diagnostic imaging experiments with multiple observations per patient, Radiology 221 (2001) 763–767.
[19] A. Luciani, A. Vignaud, M. Cavet, J.T. Nhieu, A. Mallat, L. Ruel, et al., Liver cirrhosis: intravoxel incoherent motion MR imaging–pilot study, Radiology 249 (2008) 891–899.
[20] J. Patel, E.E. Sigmund, H. Rusinek, M. Oei, J.S. Babb, B. Taouli, Diagnosis of cirrhosis with intravoxel incoherent motion diffusion MRI and dynamic contrast-enhanced MRI alone and in combination: preliminary experience, J. Magn. Reson. Imaging 31 (2010) 589–600.
[21] K. Nasu, Y. Kuroki, R. Sekiguchi, S. Nawano, The effect of simultaneous use of respiratory triggering in diffusion-weighted imaging of the liver, Magn. Reson. Med. Sci. 5 (2006) 129–136.
[22] S.Y. Kim, S.S. Lee, J.H. Byun, S.H. Park, J.K. Kim, B. Park, et al., Malignant hepatic tumors: short-term reproducibility of apparent diffusion coefficients with

breath-hold and respiratory-triggered diffusion-weighted MR imaging, Radiology 255 (2010) 815–823.
[23] H.J. Yoon, Y.K. Kim, K.T. Jang, K.T. Lee, J.K. Lee, D.W. Choi, et al., Intraductal papillary neoplasm of the bile ducts: description of MRI and added value of diffusion-weighted MRI, Abdom. Imaging 38 (2013) 1082–1090.
[24] S. Gatidis, H. Schmidt, P. Martirosian, K. Nikolaou, N.F. Schwenzer, Apparent diffusion coefficient-dependent voxelwise computed diffusion-weighted imaging: an approach for improving SNR and reducing T shine-through effects, J. Magn. Reson. Imaging 43 (2016) 824–832.
[25] S. Colagrande, L.N. Mazzoni, E. Mazzoni, S. Pradella, Effects of gadoxetic acid on quantitative diffusion-weighted imaging of the liver, J. Magn. Reson. Imaging 38 (2013) 365–370.
[26] S.E. Bouchaibi, K. Coenegrachts, M.A. Bali, J. Absil, T. Metens, C. Matos, Focal liver lesions detection: comparison of respiratory-triggering, triggering and tracking navigator and tracking-only navigator in diffusion-weighted imaging, Eur. J. Radiol. 84 (2015) 1857–1865.
[27] M. Bruegel, J. Gaa, S. Waldt, K. Woertler, K. Holzapfel, B. Kiefer, et al., Diagnosis of hepatic metastasis: comparison of respiration-triggered diffusion-weighted echo-planar MRI and five t2-weighted turbo spin-echo sequences, AJR Am. J. Roentgenol. 191 (2008) 1421–1429.
[28] B. Taouli, A. Sandberg, A. Stemmer, T. Parikh, S. Wong, J. Xu, et al., Diffusion-weighted imaging of the liver: comparison of navigator triggered and breathhold acquisitions, J. Magn. Reson. Imaging 30 (2009) 561–568.
[29] K. Holzapfel, M. Bruegel, M. Eiber, C. Ganter, T. Schuster, P. Heinrich, et al., Characterization of small (</=10 mm) focal liver lesions: value of respiratory-triggered echo-planar diffusion-weighted MR imaging, Eur. J. Radiol. 76 (2010) 89–95.